Am J Nucl Med Mol Imaging 2025;15(2):65-73
www.ajnmmi.us /ISSN:2160-8407/ajnmmi0163308

Original Article

First evaluation of [^{68}Ga]Ga-NOTA-(TMVP1)$_2$ for imaging VEGFR-3 in ovarian cancer patients

Xi Chen[1,2,3*], Fei Li[1,2*], Yao Si[1,2], Liping Han[3], Xiaoding Lou[4], Ling Xi[1,2], Jun Dai[1,2]

[1]Department of Obstetrics and Gynecology, National Clinical Research Center for Obstetrics and Gynecology, Tongji Hospital, Tongji Medical College, Huazhong University of Science and Technology, Wuhan 430034, Hubei, China; [2]Key Laboratory of Cancer Invasion and Metastasis (Ministry of Education) Hubei Key Laboratory of Tumor Invasion and Metastasis, Tongji Hospital, Tongji Medical College, Huazhong University of Science and Technology, Wuhan 430034, Hubei, China; [3]Department of Obstetrics and Gynecology, The First Affiliated Hospital of Zhengzhou University, Zhengzhou 450000, Henan, China; [4]State Key Laboratory of Biogeology and Environmental Geology, Faculty of Materials Science and Chemistry, China University of Geosciences, Wuhan 430074, Hubei, China. [*]Equal contributors.

Received January 14, 2025; Accepted March 2, 2025; Epub April 15, 2025; Published April 30, 2025

Abstract: To evaluate the safety and VEGFR-3 imaging effects of [^{68}Ga]Ga-NOTA-(TMVP1)$_2$ in ovarian cancer patients. 13 patients with ovarian cancer were recruited and underwent radionuclide imaging with [^{68}Ga]Ga-NOTA-(TMVP1)$_2$. The safety of [^{68}Ga]Ga-NOTA-(TMVP1)$_2$ was assessed in vivo (including vital signs, biochemical indices, ECG, allergic reactions, etc.) and its imaging effect on VEGFR-3 was explored. A total of 1 patient with primary ovarian cancer and 12 patients with recurrent ovarian cancer, with an age range of 41-54 years, were included in the study. 13 ovarian cancer patients had a total of 49 ^{18}F-FDG-positive lesions, 63.3% of which were positive for [^{68}Ga]Ga-NOTA-(TMVP1)$_2$. The higher expression of VEGFR-3 in [^{68}Ga]Ga-NOTA-(TMVP1)$_2$-positive ovarian cancer lesions was found by immunohistochemical staining, which was positively correlated. Meanwhile, [^{68}Ga]Ga-NOTA-(TMVP1)$_2$ is a safe radiotracer as no significant side effects have been found in the human. In conclusion, [^{68}Ga]Ga-NOTA-(TMVP1)$_2$ enables precise molecular imaging of VEGFR-3 in ovarian cancer patients with a favourable safety profile, providing a new tool for the in vivo assessment of VEGFR-3 in ovarian cancer.

Keywords: VEGFR-3, ovarian cancer, peptide, TMVP1, radiotracer

Introduction

The incidence rate of ovarian cancer has been on the rise year by year in recent years, and the death rate ranks first among malignant tumors of the female reproductive system. Ovarian cancer often has no obvious symptoms in the early stage, and about 75% of the patients are already in the advanced stages when they are diagnosed [1, 2]. Metastasis is the leading cause of death in patients with advanced ovarian cancer [3]. There are four metastatic routes of ovarian cancer, including hematogenous metastasis, lymphatic metastasis, implantation metastasis and direct invasion. The incidence of lymph node metastasis in early-stage ovarian cancer (stage I-II) is around 15%, but lymph node metastasis occurs in 70% of patients with advanced ovarian cancer, making it a potential therapeutic target [4-6].

Lymph node metastasis in ovarian cancer is closely related to lymphangiogenesis, which is strongly associated with vascular endothelial growth factor receptor 3 (VEGFR-3) (also known as Flt-4). In most solid tumors, VEGFR-3 is highly expressed in the lymphatic endothelium, and its expression is significantly higher than that in adjacent paracancerous normal tissues [7]. Yokoyama et al. found that 90% and 72% of benign and borderline ovarian tumors failed to stain for VEGFR-3 in endothelial cells adjacent to tumor cells, respectively [8]. However, 57% of ovarian carcinomas stained positively for VEGFR-3 in endothelial cells adjacent to the carcinoma. The expression of VEGFR-3 in ovarian tumors correlates with their benignity and malignancy, suggesting that VEGFR-3 has an important role in the development of ovarian cancer. After co-culturing lymphatic endothelial cells with ovarian cancer cells, the migration and metastasis of cancer cells were significantly enhanced, which might be triggered by activating the MMP-9/TIMP-2 pathway [9]. Overexpression of VEGFR-3 in ovarian cancer was found to correlate with debulking status and positive response to chemotherapy, and progression-free survival was significantly longer in women with low VEGFR-3 expression than in women with high VEGFR-3 expression [10]. In all, overexpression of VEGFR-3 reflects the aggressiveness of ovarian carcinoma spread and has a predictive value for identifying high-risk patients with poor prognosis. VEGFR-3 is known to be involved in tumorigenesis and lymphangiogenesis, and thus has the potential to be a molecular target for cancer therapy. Babaei et al. used a VEGFR-3 inhibitor to treat ovarian cancer and found that it increased cell cycle arrest and promoted apoptosis in OVCAR3 and SKOV3 cells by inhibiting the ERK-2 and AKT signaling pathways [11]. Cediranib, a broad-acting tyrosine kinase inhibitor (TKI), was also able to significantly inhibit ovarian cancer metastasis [12]. Therefore, monitoring VEGFR-3 expression in ovarian cancer is useful for assessing patient prognosis and guiding VEGFR-3-targeted therapy.

A monoclonal antibody mF4-31C1-labeled radiotracer was constructed for tracer imaging of VEGFR-3 in ovarian cancer by Huhtala et al. [13]. The antibody-labeled radiotracer required 48 hours after injection to be detected in ovarian cancer tissue, and the uptake rate was only 5.77 ± 0.62 %ID/g. Peptide-based radiotracers have the advantage of rapid imaging and are typically ready for manipulation 30-60 minutes after injection [14, 15]. Li et al. screened a peptide, WHWLPNLRHYAS, that binds specifically to VEGFR-3 with an affinity constant of 174.8 ± 31.1 μg/mL between them [16]. Further, our group screened a peptide with high affinity for VEGFR-3, TMVP1 [17]. TMVP1 has an affinity for VEGFR-3 of 6.73 μM/mL and has demonstrated the ability of this peptide radiotracer to image VEGFR-3 in patients with ovarian and cervical cancer. Nanoparticles prepared as fluorescent tracers using TMVP1 can be used for imaging and treatment of primary tumors and metastatic tumors in lymph nodes [18]. To further enhance the potential application of TMVP1, we designed it as a dimer ([^{68}Ga]Ga-NOTA-(TMVP1)$_2$) and demonstrated that the dimeric peptide had better VEGFR-3 targeting compared to the monomeric peptide [19]. In this study, we used [^{68}Ga]Ga-NOTA-(TMVP1)$_2$ radiotracer for the first time to assess the level of VEGFR-3 expression in patients with ovarian cancer, providing a new potential tool for stratifying ovarian cancer patients based on VEGFR-3 expression.

Methods

Participant enrollment

The clinical investigation was registered with the Chinese Clinical Trial Registry (ChiCTR-DOD-17012458) and received approval from the Institutional Review Board (IRB) of Peking Union Medical College Hospital, Chinese Academy of Medical Sciences (Ethics number ZS-1128). Written informed consent was obtained from all participants. The study adhered to ethical guidelines outlined by institutional and national research committees, as well as the principles of the Declaration of Helsinki (1964) and its subsequent amendments.

Eligible participants were diagnosed with either primary ovarian cancer or postoperative recurrence, aged ≥18 years, and capable of providing informed consent. Exclusion criteria included pregnancy, lactation, severe hepatic/renal dysfunction (glomerular filtration rate < 60 mL/min/1.73 m^2 or hepatic enzymes ≥2× upper normal limit), hypersensitivity to radiographic agents, claustrophobia, or psychiatric conditions. Vital parameters (e.g., blood pressure, heart rate), physical examinations, electrocardiograms, hematological profiles, and hepatic/renal function markers were documented before and after intravenous administration of [^{68}Ga]Ga-NOTA-(TMVP1)$_2$.

Imaging protocol

In contrast to [^{18}F]F-FDG PET/CT protocols requiring prescan fasting, no dietary restrictions were imposed for this study. Participants were instructed to empty their bladders prior to imaging. Following intravenous injection of [^{68}Ga]Ga-NOTA-(TMVP1)$_2$, whole-body PET scans were conducted 30-45 minutes post-administration using 5-6 bed positions (10-minute acquisition per bed), spanning from the skull to mid-femur. A low-dose CT scan (120 kV, 35 mA, 3 mm slice thickness, 512×512 matrix, 70 cm FOV) preceded PET imaging for attenuation correction. Two nuclear medicine specialists independently delineated regions of interest (ROIs) on co-registered CT images to quantify maximum and average standardized uptake values (SUV_{max}/SUV_{mean}) for lesions and organs.

Immunohistochemical analysis

VEGFR-3 expression in ovarian cancer tissues was evaluated via immunohistochemistry (IHC). Tissue specimens underwent fixation in 4% paraformaldehyde, paraffin embedding, and sectioning. After deparaffinization and rehydration, endogenous peroxidase activity was blocked with 3% H_2O_2 (20 minutes). Sections were treated with bovine serum albumin to minimize nonspecific binding, followed by overnight incubation at 4°C with anti-VEGFR-3 primary antibody (BioLegend, 356202, 1:100 dilution). Horseradish peroxidase-conjugated anti-mouse IgG secondary antibody was applied (37°C, 30 minutes), with subsequent diaminobenzidine staining and hematoxylin counterstaining. Three blinded observers independently scored staining intensity and VEGFR-3-positive cell percentages.

Statistical evaluation

PET image processing was performed using Siemens Multi-Modality Workplace (MMWP). ROIs for normal tissues and lesions were manually defined, with the workstation calculating radioactivity concentrations and SUVs. GraphPad Prism (v5.0) facilitated statistical analyses and time-activity curve generation. Lesion uptake characteristics of [^{68}Ga]Ga-NOTA-(TMVP1)$_2$ and [^{18}F]F-FDG were evaluated by experienced radiologists. Data are presented as mean ± standard deviation. Intergroup comparisons employed Student's t-test or one-way ANOVA, with $P < 0.05$ considered statistically significant.

Results

Clinical characteristics of the patients

Between October 2016 and April 2017, 13 ovarian cancer patients (**Table 1**) were enrolled in the study. The ages of the 13 patients ranged from 32 to 54 years, with a mean age of 46.5 years. All patients weighed between 44 and

Table 1. Information of the patient

No.	Age	Gender	Weight (kg)	Clinical diagnosis
1	45	Female	75	Recurrent ovarian cancer
2	49	Female	52	Recurrent ovarian cancer
3	44	Female	64	Recurrent ovarian cancer
4	32	Female	47	Recurrent ovarian cancer
5	42	Female	60	Primary ovarian cancer
6	51	Female	60	Recurrent ovarian cancer
7	52	Female	55	Recurrent ovarian cancer
8	41	Female	58	Recurrent ovarian cancer
9	54	Female	44	Recurrent ovarian cancer
10	47	Female	61	Recurrent ovarian cancer
11	50	Female	50	Recurrent ovarian cancer
12	49	Female	46	Recurrent ovarian cancer
13	49	Female	75	Recurrent ovarian cancer

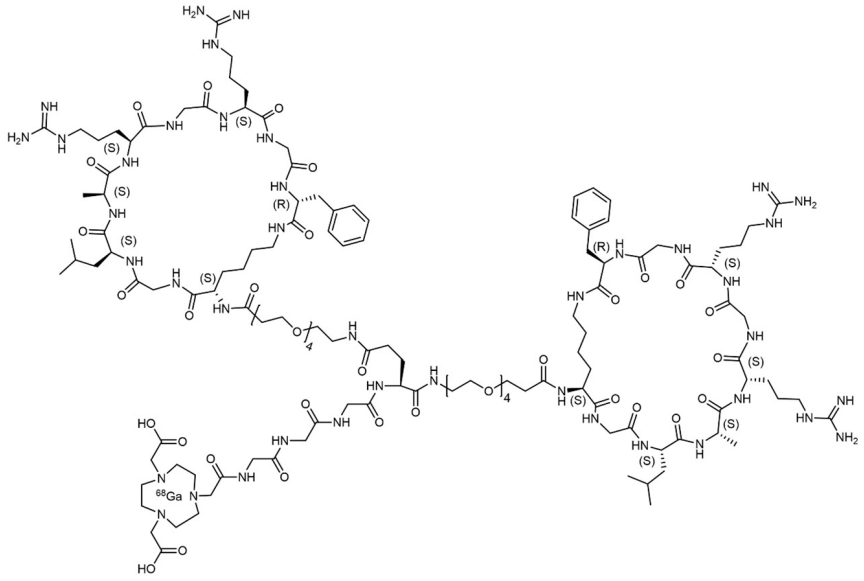

Figure 1. Chemical structure of [^{68}Ga]Ga-NOTA-(TMVP1)$_2$.

75 kg, with a mean weight of 57.5 kg, and no patient was overweight or underweight. Except for one patient who had primary ovarian cancer, all 12 patients had recurrent ovarian cancer after surgery.

PET/CT imaging of [^{68}Ga]Ga-NOTA-(TMVP1)$_2$

The structural formula of [^{68}Ga]Ga-NOTA-(TMVP1)$_2$ is shown in **Figure 1**, and it has a radiochemical purity of over 95%. All ovarian cancer patients included in the study underwent [^{18}F]F-FDG scans, and identified as having 1 or more positive lesions. 13 ovarian cancer patients were included in the study with a total of 44 [^{18}F]F-FDG positive lesions. Of these 44 ^{18}F-FDG-positive lesions, 26 were positive for [^{68}Ga]Ga-NOTA-(TMVP1)$_2$. Another 18 lesions were positive for ^{18}F-FDG but negative for [^{68}Ga]Ga-NOTA-(TMVP1)$_2$ (**Table 2**). Patient #2 was a patient with recurrent ovarian cancer, as shown in **Figure 2**, and [^{18}F]F-FDG showed recurrent ovarian cancer lesions in both the pelvis and vaginal stump. The radioactivity of the right pelvic intestinal surface metastases was significantly increased at [^{18}F]F-FDG, while the radioactivity of [^{68}Ga]Ga-NOTA-(TMVP1)$_2$ reached 2.53 for SUV$_{max}$ and 1.53 for SUV$_{mean}$ (**Figure 2A**). For the recurrent cancer of the vaginal stump in patient #2, the [^{68}Ga]Ga-NOTA-(TMVP1)$_2$ had an SUV$_{max}$ of 1.57 and an SUV$_{mean}$ of 1.07, thus judging that the lesion was also positive (**Figure 2B**). Patient #4 had recurrent ovarian cancer and CT showed significant thickening of the gastric wall in the greater curvature of the stomach (**Figure 3**). [^{18}F]F-FDG uptake was positive in this lesion with a SUV$_{max}$ of 2.2. Meanwhile, the uptake of [^{68}Ga]Ga-NOTA-(TMVP1)$_2$ by the lesion was significantly higher, with increased radioactivity in the lesion, SUV$_{max}$ 2.5 and SUV$_{mean}$ 1.85. Patient #7, [^{18}F]F-FDG PET/CT showed multiple ovarian cancer metastases in the liver (**Figure 4**). These metastases all had higher uptake of [^{18}F]F-FDG compared to the surrounding normal liver tissue. [^{68}Ga]Ga-NOTA-(TMVP1)$_2$ had a range of 2.64-3.93 for SUV$_{max}$ and 1.13-1.66 for SUV$_{mean}$ in metastatic cancer of the liver. The uptake of [^{68}Ga]Ga-NOTA-(TMVP1)$_2$ by these metastases was low relative to normal liver tissue, but increased relative to muscle, and was therefore nonetheless assessed as positive.

Association of [^{68}Ga]Ga-NOTA-(TMVP1)$_2$ uptake and expression of VEGFR-3

Of the 13 patients with ovarian cancer, 5 underwent surgery. Independent diagnosis was made by two pathologists and confirmed the pathologic type of ovarian plasmacytoid cystadenocarcinoma in all five patients. Immunohistochemical staining was used to detect the expression level of VEGFR-3 in a total of 15 ovarian cancer tissues from these five patients (**Figure 5**). Immunohistochemical results showed that these ovarian cancer lesions had varying degrees of VEGFR-3 expression, and 70% of the lesions were determined to be VEGFR-3 positive. Also, these VEGFR-3-positive ovarian cancer lesions were positive for [^{68}Ga]Ga-NOTA-(TMVP1)$_2$ uptake.

Discussion

Ovarian cancer is the cancer with the highest mortality rate among gynaecological malignancies, and currently, its standard clinical treatment options are tumor cytoreduction and chemotherapy [19, 20]. With the arrival of

Table 2. Uptake of [^{68}Ga]Ga-NOTA-(TMVP1)$_2$ by ovarian cancer lesions

No.	Site of lesion	[^{68}Ga]Ga-NOTA-(TMVP1)$_2$		
		SUV_{max}	SUV_{mean}	Results
1	Liver	5.91	4.60	Negative
2	Pelvis	2.53	1.53	Positive
	Vaginal stump	1.57	1.07	Positive
	Retroperitoneal lymph nodes	1.16	0.80	Negative
3	Pelvis	2.84	2.01	Positive
	Liver	6.06	4.69	Negative
4	Lesser curvature of the stomach	2.50	1.85	Positive
	Greater curvature of the stomach	2.06	1.35	Positive
5	Uterine adnexa	2.79	1.67	Positive
	Pelvis	1.59	1.18	Positive
	Retroperitoneal lymph nodes	2.04	1.15	Positive
6	Para-abdominal aortic lymph nodes	1.58	1.06	Positive
		1.42	1.02	Positive
	Mesenteric lymph nodes	0.71	0.68	Negative
	Pelvis	0.98	0.52	Negative
7	Liver	3.93	1.66	Positive
		2.64	1.13	Positive
	Lung	1.21	0.87	Negative
	Para-abdominal aortic lymph nodes	1.94	1.12	Positive
	Pelvis	1.28	0.92	Negative
		0.94	0.62	Negative
		0.28	0.18	Negative
8	Splenic hilum	1.14	0.85	Positive
9	Cervical lymph nodes	1.84	1.22	Positive
	Paraesophageal	1.86	1.23	Negative
	Pancreas	2.71	1.58	Positive
10	Liver	3.93	3.05	Positive
		5.53	4.15	Positive
		5.90	4.60	Negative
	Pelvis	1.12	0.86	Negative
		1.03	0.92	Negative
		1.95	1.05	Negative
11	Hepatic peritoneum	4.03	2.47	Negative
	Pelvis	2.22	1.69	Positive
		2.32	1.85	Positive
		2.88	2.12	Positive
12	Spleen	2.88	1.59	Negative
13	Vaginal stump	3.32	1.83	Positive
	Axillary lymph nodes	1.74	1.11	Negative
		1.95	1.28	Negative
	Retroperitoneal lymph nodes	1.98	1.06	Positive
		2.51	1.52	Positive
	Abdominal incision	2.87	1.61	Positive
	Inguinal lymph nodes	2.42	1.51	Positive
Summary	44 lesions			59.1% (Positive)

precision medicine, molecular targeted therapy has gradually entered people's vision and plays an increasingly important role in the field of anti-ovarian cancer [21, 22]. Molecular targeted therapy is to intervene in the key targets in the process of tumor development and other important effects, such as bevacizumab for anti-angiogenic therapy and so on [23-25]. In general, the status of ovarian cancer target molecules needs to be evaluated before targeted therapy is administered; for example, the application of PARP inhibitors is predicated on a mutation in the BRCA gene [26-28]. VEGFR-3 has been reported to be closely associated with lymphangiogenesis, as well as lymphatic metastasis, in ovarian cancer [7, 12]. The use of the VEGFR inhibitor Cediranib significantly inhibited ovarian cancer metastasis and is a potential treatment. Significant inhibition of tumour growth as well as metastasis was achieved by adenovirus-based anti-VEGFR1-3 combination therapy [29]. IHC staining allows assessment of VEGFR-3 expression status in isolated ovarian cancer tissues, whereas molecular assessment in vivo requires imaging techniques such as PET/CT.

The variety of VEGFR radiotracers is vast, and the main part of the tracer usually consists of small molecules, antibodies, peptides, and proteins [30-38]. Yang et al. prepared a radiotracer, [^{18}F]-VEGFR, using the small molecule compound diZD [30]. [^{18}F]-VEGFR PET showed significantly lower cardiac background signal compared with [^{18}F]-FDG PET, improved imaging sensitivity for lung abnormalities, and demonstrated potential application in noninvasive detection of pulmonary arterial hypertension and monitoring its progression. Small molecule radiotracers typically have a fast in vivo distribution rate and can be rapidly cleared from non-target tissues, thereby reducing background noise, but due to their small size, small molecules may lack sufficient specificity to readily bind to non-target sites [31]. Radiotracers based on VEGF fragments or VEGFR antibodies are also a promising tool for molecular visualization of VEGFR [32, 33]. Antibodies or proteins can provide a high degree of selectivity and affinity for specific antigenic epitopes, but antibodies and proteins are larger, diffuse slower, and are also cleared slow-

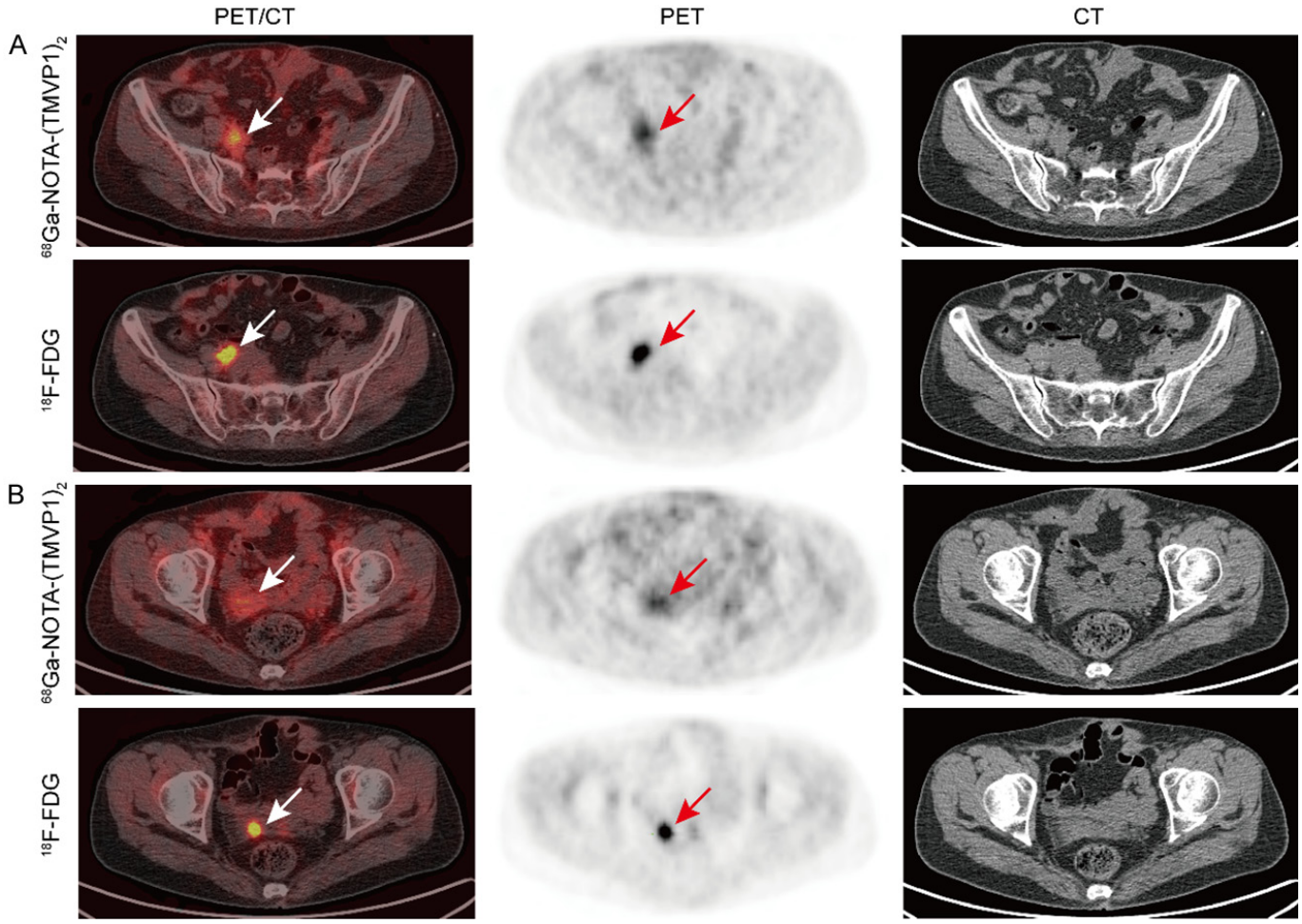

Figure 2. Uptake of [^{68}Ga]Ga-NOTA-(TMVP1)$_2$ by patient #2. A. Increased radioactivity uptake of [^{68}Ga]Ga-NOTA-(TMVP1)$_2$ by right pelvic intestinal surface metastases, SUV_{max} = 2.53, SUV_{mean} = 1.53. B. Increased uptake of [^{68}Ga]Ga-NOTA-(TMVP1)$_2$ by vaginal stump lesions, SUV_{max} = 1.57, SUV_{mean} = 1.07. Red arrows indicate ovarian cancer lesions.

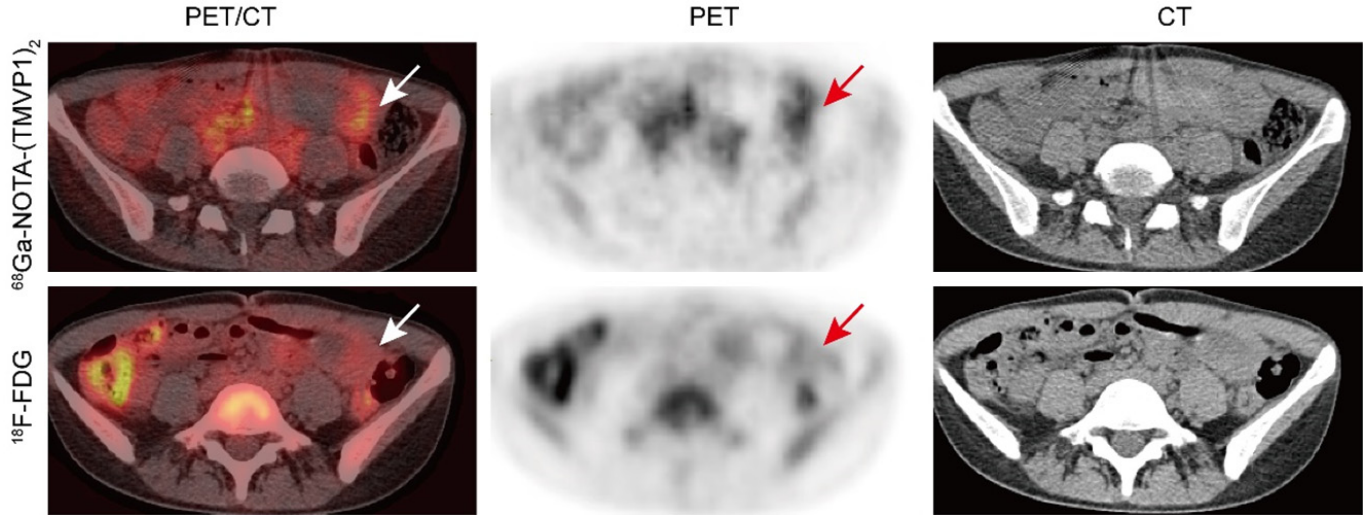

Figure 3. Uptake of [^{68}Ga]Ga-NOTA-(TMVP1)$_2$ by patient #4. CT showed thickening of the gastric wall at the greater curvature of the stomach. The uptake of ^{18}F-FDG was increased at the lesion, SUV_{max} 2.2. The [^{68}Ga]Ga-NOTA-(TMVP1)$_2$ radioactivity was increased at the lesion, SUV_{max} 2.5, SUV_{mean} 1.85.

er from non-targeted tissues, which may result in higher background noise [34-36]. Peptides are intermediate between small molecules and antibodies, finding a better balance between specificity, penetration ability and in

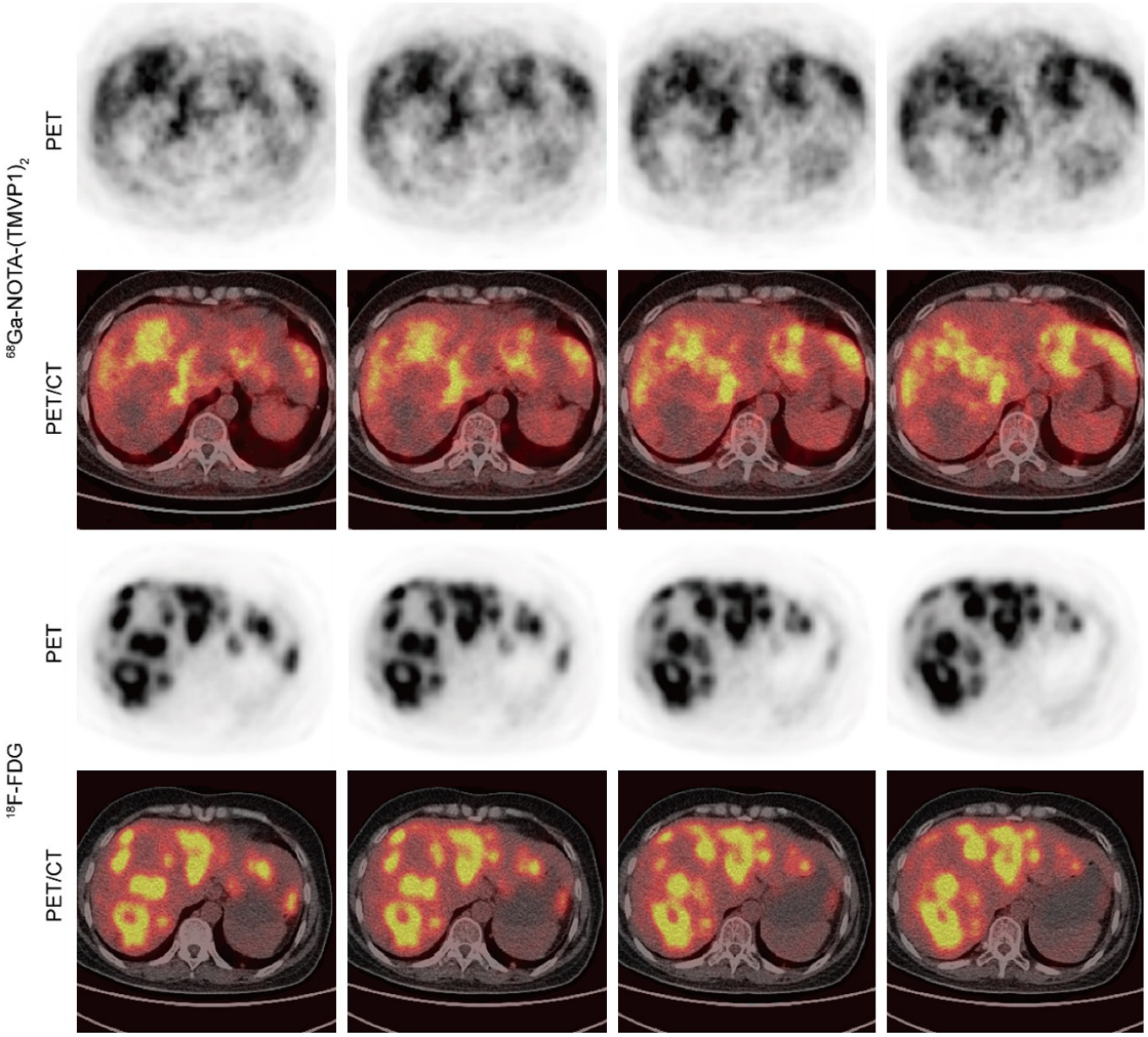

Figure 4. Uptake of [^{68}Ga]Ga-NOTA-(TMVP1)$_2$ by ovarian cancer liver metastases. ^{18}F-FDG PET/CT images showed enlarged liver and increased radioactivity of ovarian cancer liver metastases. The uptake of [^{68}Ga]Ga-NOTA-(TMVP1)$_2$ by normal liver tissue had a SUV_{max} of 5.55 and a SUV_{mean} of 3.45. The uptake of [^{68}Ga]Ga-NOTA-(TMVP1)$_2$ by ovarian cancer liver metastases was low, with a SUV_{max} of 2.64-3.93 and a SUV_{mean} of 1.13-1.66.

vivo half-life, and are also often used for in vivo visualization of VEGFR [37, 38].

TMVP1 is a target peptide that we have previously screened for VEGFR-3. The core sequence of TMVP1 is LARGR, which was cyclized to have an affinity of 6.73×10^{-6} M for VEGFR-3. The TMVP1-based radiotracer ^{68}Ga-DOTA-TMVP1 was clinically tested in five patients with ovarian and three with cervical cancer, and the results showed that it had a favorable safety profile and VEGFR-3 visualization [17]. To further optimise and enhance the affinity of TMVP1 for VEGFR-3, we designed a radionuclide probe based on TMVP1 dimer, [^{68}Ga]Ga-NOTA-(TMVP1)$_2$ [39]. Its affinity for VEGFR-3 was almost twice as high as that of TMVP1, reaching 3.74×10^{-6} M. In 5 healthy volunteers and 8 patients with cervical cancer, [^{68}Ga]Ga-NOTA-(TMVP1)$_2$ demonstrated a favourable safety profile, with no side effects or allergies noted. In patients with cervical cancer, 81.8% of lesions [^{68}Ga]Ga-NOTA-(TMVP1)$_2$ showed medium- and high-intensity radiation signals. This molecular imaging agent is able to accurately assess the VEGFR-3 status of cervical cancer and provides a good tool for anti-VEGFR-3 therapy in cervical cancer. In this study, we used [^{68}Ga]Ga-NOTA-(TMVP1)$_2$ to evaluate VEGFR-3 in a total of 44 lesions in 9 ovarian cancer patients. The results showed that 26 out of 44 ovarian cancer lesions had positive VEGFR-3 expression. This may have the following implica-

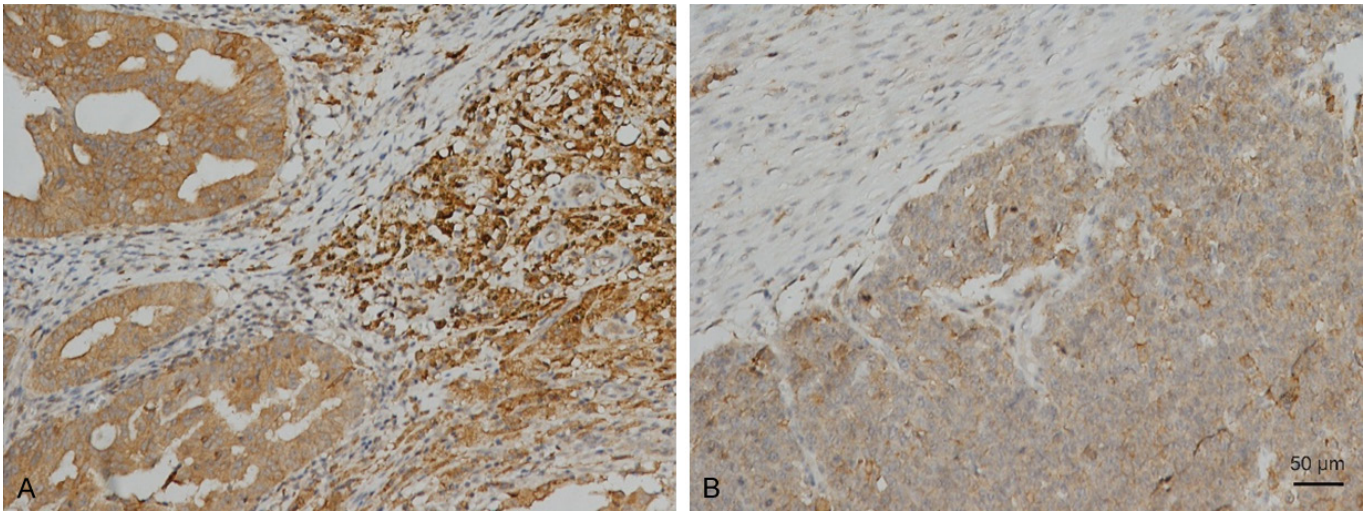

Figure 5. A. VEGFR-3 expression in the primary lesion of ovarian cancer. B. VEGFR-3 expression in ovarian cancer liver metastases.

tions and impact on the management of ovarian cancer. A clinical study shows that anti-VEGFR-3 treatment with small molecule inhibitors can be effective [40]. Precise assessment of VEGFR-3 expression levels in ovarian cancer using [^{68}Ga]Ga-NOTA-(TMVP1)$_2$ could provide more information for anti-VEGFR-3 therapy. It has also been suggested that overexpression of VEGFR-3 correlates with the level of differentiation, response to chemotherapy, and prognosis of ovarian cancer [10], which implies that [^{68}Ga]Ga-NOTA-(TMVP1)$_2$ can achieve the ability to provide guidance for staging and treatment of ovarian cancer. The aim of this study is to provide a preliminary assessment of the role of [^{68}Ga]Ga-NOTA-(TMVP1)$_2$ in imaging and analysing VEGFR-3 in ovarian cancer, as well as its safety in vivo. This study confirms the feasibility of VEGFR-3 imaging assessment, but there are some limitations. The most important point is that the number of cases is only 13, which is not enough to illustrate the accuracy of the [^{68}Ga]Ga-NOTA-(TMVP1)$_2$ assessment. Second, the positive correlation between the molecular level of VEGFR-3 and the level of radioactivity detected by PET cannot be affirmed due to the missing part of the tissue specimen.

Conclusion

In this study, we used [^{68}Ga]Ga-NOTA-(TMVP1)$_2$ to assess VEGFR-3 status in 13 ovarian cancer patients. Twenty-six out of a total of 44 ovarian cancer lesions showed positivity for VEGFR-3, and these lesions exhibited moderate-high radioactivity. The expression level of VEGFR-3 in five ovarian cancer patients was detected by immunohistochemical staining and the association between radioactivity and VEGFR-3 was established. In conclusion, [^{68}Ga]Ga-NOTA-(TMVP1)$_2$ provides a new tool for VEGFR-3 in ovarian cancer patients.

Acknowledgements

This study was funded by the National Natural Science Foundation of China (81802608, 22104040 and 82272628), Knowledge Innovation Program of Wuhan-Shuguang Project (280) and The Co-operation Research Plan of Medical Science and Technology of Henan Province (LHGJ20220415).

Written informed consent to use data for research purposes was obtained from all patients.

Disclosure of conflict of interest

None.

Address correspondence to: Jun Dai and Ling Xi, Department of Obstetrics and Gynecology, National Clinical Research Center for Obstetrics and Gynecology, Tongji Hospital, Tongji Medical College, Huazhong University of Science and Technology, Wuhan 430034, Hubei, China. E-mail: jundai@tjh.tjmu.edu.cn (JD); lxi@tjh.tjmu.edu.cn (LX)

References

[1] Webb PM and Jordan SJ. Global epidemiology of epithelial ovarian cancer. Nat Rev Clin Oncol 2024; 21: 389-400.
[2] Lheureux S, Braunstein M and Oza AM. Epithelial ovarian cancer: evolution of management in the era of precision medicine. CA Cancer J Clin 2019; 69: 280-304.
[3] Yousefi M, Dehghani S, Nosrati R, Ghanei M, Salmaninejad A, Rajaie S, Hasanzadeh M and Pasdar A. Current insights into the metastasis of epithelial ovarian cancer - hopes and hurdles. Cell Oncol 2020; 43: 515-538.
[4] Balbi G, Manganaro MA, Monteverde A, Landino I, Franzese C and Gioia F. Ovarian cancer: lymph node metastases. Eur J Gynaecol Oncol 2009; 30: 289-291.
[5] Kleppe M, Wang T, Van Gorp T, Slangen BF, Kruse AJ and Kruitwagen RF. Lymph node metastasis in stages I and II ovarian cancer: a review. Gynecol Oncol 2011; 123: 610-614.
[6] Nomura H, Tsuda H, Susumu N, Fujii T, Banno K, Kataoka F, Tominaga E, Suzuki A, Chiyoda T and Aoki D. Lymph node metastasis in grossly apparent stages I and II epithelial ovarian cancer. Int J Gynecol Cancer 2010; 20: 341-345.

[7] Smith NR, Baker D, James NH, Ratcliffe K, Jenkins M, Ashton SE, Sproat G, Swann R, Gray N, Ryan A, Jürgensmeier JM and Womack C. Vascular endothelial growth factor receptors VEGFR-2 and VEGFR-3 are localized primarily to the vasculature in human primary solid cancers. Clin Cancer Res 2010; 16: 3548-3561.

[8] Yokoyama Y, Charnock-Jones DS, Licence D, Yanaihara A, Hastings JM, Holland CM, Emoto M, Umemoto M, Sakamoto T, Sato S, Mizunuma H and Smith SK. Vascular endothelial growth factor-D is an independent prognostic factor in epithelial ovarian carcinoma. Brit J Cancer 2003; 88: 237-244.

[9] Yang S, Zhu X, Cai L, Cheng H, Zhao R, Wang H, Zhao H and Wang Z. Role of tumor-associated lymphatic endothelial cells in metastasis: a study of epithelial ovarian tumor in vitro. Cancer Sci 2010; 101: 679-685.

[10] Klasa-Mazurkiewicz D, Jarząb M, Milczek T, Lipińska B and Emerich J. Clinical significance of VEGFR-2 and VEGFR-3 expression in ovarian cancer patients. Pol J Pathol 2011; 62: 31-40.

[11] Babaei Z, Panjehpour M, Parsian H and Aghaei M. SAR131675 exhibits anticancer activity on human ovarian cancer cells through inhibition of VEGFR-3/ERK1/2/AKT signaling pathway. Cell Signal 2023; 111: 110856.

[12] Decio A, Taraboletti G, Patton V, Alzani R, Perego P, Fruscio R, Jürgensmeier JM, Giavazzi R and Belotti D. Vascular endothelial growth factor c promotes ovarian carcinoma progression through paracrine and autocrine mechanisms. Am J Pathol 2014; 184: 1050-1061.

[13] Huhtala T, Laakkonen P, Sallinen H, Ylä-Herttuala S and Närvänen A. In vivo SPECT/CT imaging of human orthotopic ovarian carcinoma xenografts with 111In-labeled monoclonal antibodies. Nucl Med Biol 2010; 37: 957-964.

[14] Kręcisz P, Czarnecka K, Królicki L, Mikiciuk-Olasik E and Szymański P. Radiolabeled peptides and antibodies in medicine. Bioconjug Chem 2021; 32: 25-42.

[15] Opalinska M, Hubalewska-Dydejczyk A and Sowa-Staszczak A. Radiolabeled peptides: current and new perspectives. Q J Nucl Med Mol Imaging 2017; 61: 153-167.

[16] Shi LF, Wu Y and Li CY. Identification of high-affinity VEGFR3-binding peptides through a phage-displayed random peptide library. J Gynecol Oncol 2015; 26: 327-335.

[17] Li F, Zhang Z, Cai J, Chen X, Zhou Y, Ma X, Dong Q, Li F and Xi L. Primary preclinical and clinical evaluation of ^{68}Ga-DOTA-TMVP1 as a novel VEGFR-3 PET imaging radiotracer in gynecological cancer. Clin Cancer Res 2020; 26: 1318-1326.

[18] Wang X, Dai G, Jiang G, Zhang D, Wang L, Zhang W, Chen H, Cheng T, Zhou Y, Wei X, Li F, Ma D, Tan S, Wei R and Xi L. A TMVP1-modified near-infrared nanoprobe: molecular imaging for tumor metastasis in sentinel lymph node and targeted enhanced photothermal therapy. J Nanobiotechnology 2023; 21: 130.

[19] Konstantinopoulos PA, Matulonis UA. Clinical and translational advances in ovarian cancer therapy. Nat Cancer 2023; 4: 1239-1257.

[20] Wang L, Wang X, Zhu X, Zhong L, Jiang Q, Wang Y, Tang Q, Li Q, Zhang C, Wang H and Zou D. Drug resistance in ovarian cancer: from mechanism to clinical trial. Mol Cancer 2024, 23: 66.

[21] Morand S, Devanaboyina M, Staats H, Stanbery L and Nemunaitis J. Ovarian cancer immunotherapy and personalized medicine. Int J Mol Sci 2021; 22: 6532.

[22] Diab Y and Muallem MZ. Therapy in ovarian cancer. A comprehensive systematic review of literature. Anticancer Res 2017; 37: 2809-2815.

[23] Nakai H and Matsumura N. The roles and limitations of bevacizumab in the treatment of ovarian cancer. Int J Clin Oncol 2022; 27: 1120-1126.

[24] Kuroki L and Guntupalli SR. Treatment of epithelial ovarian cancer. BMJ 2022; 371: m3773.

[25] Richardson DL, Eskander RN and O'Malley DM. Advances in ovarian cancer care and unmet treatment needs for patients with platinum resistance: a narrative review. JAMA Oncol 2023; 9: 851-859.

[26] Mirza MR, Coleman RL, González-Martín A, Moore KN, Colombo N, Ray-Coquard I and Pignata S. The forefront of ovarian cancer therapy: update on PARP inhibitors. Ann Oncol 2020; 31: 1148-1159.

[27] Moschetta M, George A, Kaye SB and Banerjee S. BRCA somatic mutations and epigenetic BRCA modifications in serous ovarian cancer. Ann Oncol 2016; 27: 1449-1455.

[28] Wu Y, Xu S, Cheng S, Yang J and Wang Y. Clinical application of PARP inhibitors in ovarian cancer: from molecular mechanisms to the current status. J Ovarian Res 2023; 16: 6.

[29] Sallinen H, Anttila M, Narvainen J, Koponen J, Hamalainen K, Kholova I, Heikura T, Toivanen P, Kosma VM, Heinonen S, Alitalo K and Yla-Herttuala S. Antiangiogenic gene therapy with soluble VEGFR-1, -2, and -3 reduces the growth of solid human ovarian carcinoma in mice. Mol Ther 2009; 17: 278-284.

[30] Yang Z, Li F, Thandavarayan RA, Natarajan K, Martin DR, Li Z and Guha A. Early detection of pulmonary arterial hypertension through [^{18}F] positron emission tomography imaging with a vascular endothelial receptor small molecule. Pulm Circ 2024; 14: e12393.

[31] Vāvere AL and Scott PJH. Clinical applications of small-molecule PET radiotracers: current progress and future outlook. Semin Nucl Med 2017; 47: 429-453.

[32] Mason CA, Carter LM, Mandleywala K, de Souza Franca PD, Meyer JP, Mamun T, Backer JM, Backer MV, Reiner T and Lewis JS. Imaging early-stage metastases using an ^{18}F-labeled VEGFR-1-specific single chain VEGF mutant. Mol Imaging Biol 2021; 23: 340-349.

[33] Novy Z, Janousek J, Barta P, Petrik M, Hajduch M and Trejtnar F. Preclinical evaluation of anti-VEGFR2 monoclonal antibody ramucirumab labelled with zirconium-89 for tumour imaging. J Labelled Comp Radiopharm 2021; 64: 262-270.

[34] Alluri SR, Higashi Y and Kil KE. PET imaging radiotracers of chemokine receptors. Molecules 2021; 26: 5174.

[35] Kręcisz P, Czarnecka K, Królicki L, Mikiciuk-Olasik E and Szymański P. Radiolabeled peptides and antibodies in medicine. Bioconjug Chem 2021; 32: 25-42.

[36] Meyer JP, Edwards KJ, Kozlowski P, Backer MV, Backer JM and Lewis JS. Selective imaging of VEGFR-1 and VEGFR-2 using 89Zr-labeled single-chain VEGF mutants. J Nucl Med 2016; 57: 1811-1816.

[37] Hu K, Shang J, Xie L, Hanyu M, Zhang Y, Yang Z, Xu H, Wang L and Zhang MR. PET imaging of VEGFR with a novel 64Cu-labeled peptide. ACS Omega 2020; 5: 8508-8514.

[38] Barta P, Kamaraj R, Kucharova M, Novy Z, Petrik M, Bendova K, Hajduch M, Pavek P and Trejtnar F. Preparation, in vitro affinity, and in vivo biodistribution of receptor-specific 68Ga-labeled peptides targeting vascular endothelial

growth factor receptors. Bioconjug Chem 2022; 33: 1825-1836.

[39] Chen X, Zhang Z, Wang L, Zhang J, Zhao T, Cai J, Dang Y, Guo R, Liu R, Zhou Y, Wei R, Lou X, Xia F, Ma D, Li F, Dai J, Li F and Xi L. Homodimeric peptide radiotracer [^{68}Ga]Ga-NOTA-$(TMVP1)_2$ for VEGFR-3 imaging of cervical cancer patients. Eur J Nucl Med Mol Imaging 2024; 51: 2338-2352.

[40] Matulonis UA, Berlin S, Ivy P, Tyburski K, Krasner C, Zarwan C, Berkenblit A, Campos S, Horowitz N, Cannistra SA, Lee H, Lee J, Roche M, Hill M, Whalen C, Sullivan L, Tran C, Humphreys BD and Penson RT. Cediranib, an oral inhibitor of vascular endothelial growth factor receptor kinases, is an active drug in recurrent epithelial ovarian, fallopian tube, and peritoneal cancer. J Clin Oncol 2009; 27: 5601-5606.